Parametric and geometric PDE-based models for automatic image segmentation

T. Barbu

Abstract. This research paper represents a survey describing some high-level mathematical models for digital image segmentation. They are divided into parametric and geometric partial differential equation (PDE)-based segmentation models. So, various parametric Active Contour models, which are based on PDE variational schemes, are surveyed first. The geometric, or geodesic, Active Contour models are presented next. They represent variational image segmentation solutions that combine successfully some parametric Active Contours to level-set functions in order to achieve an improved image partitioning. Our own contributions in this image analysis field are also discussed here.

M.S.C. 2010: 68U10, 94A08, 93E11, 60G35, 35A15, 35-XX, 35Kxx, 35K10, 35K55, 35Lxx, 35L70, 14Jxx.
Key words: automatic image segmentation; PDE variational models; energy minimization; parametric active contour; geometric active contour; level sets.

1 Introduction

Digital image segmentation represents an important image analysis domain whose goal is to obtain a meaningful partition of each analyzed image. Such a segmentation process generates multiple image segments, each of them having the property that its pixels share certain characteristics, being similar with respect to some computed property, such as color, intensity or texture [28].

Image segmentation has many important computer vision application areas. They include object detection and tracking [18], image object recognition, biometric authentication, image and video indexing and retrieval [11], video segmentation [24], video surveillance [29] and the medical imaging [27].

Various image segmentation techniques have been developed in the last decades. These segmentation methods could be grouped in the following main categories: thresholding-based algorithms, edge-based methods [21], histogram-based techniques [28], pixel clustering-based approaches [10, 19], motion-based solutions [23], compression-based schemes [25], graph partitioning methods [20] and partial differential equation (PDE)-based techniques.

Applied Sciences, Vol. 24, 2022, pp. 1-11.

The PDE-based image segmentation approaches are those surveyed in this paper. We have performed a high amount of research in the PDE-based image processing and analysis domains in the last 15 years [4, 8, 9]. The PDE-based image segmentation field has been also approached successfully by us, several segmentation techniques being developed [2, 5].

The most popular PDE-based image segmentation models are based on curve propagation and have a variational character, since they perform minimizations of some energy-based functionals. They can be divided into two main categories: parametric and geometric models.

The parametric PDE-based image segmentation techniques are described in the following section. Then, the geometric PDE-based segmentation models will be described in the third section. Our own contributions in this area, representing nonlinear PDE-based image segmentation solutions, are also discussed in this paper. This survey article ends with a section of conclusions and a list of references.

2 Parametric PDE-based segmentation models

As we have already mentioned, the PDE-based image segmentation techniques could be represented as variational (energy-based) models that minimize some properly chosen energy cost functionals. The Active Contour models, also called *snakes*, represent such energy minimizing-based image segmentation frameworks. Introduced by Michael Kass, Andrew Witkin and Demetri Terzopoulos in 1988 [22], the snakes represent deformable splines influenced by constraint and image forces that pull them towards the contours of the objects and internal forces which resist deformation.

These deformable models that detect the boundaries of the image objects are grouped in two categories: parametric and geometric active contours. The parametric models, which are discussed in this section, represent contours explicitly as parameterized curves [22].

A parametric active contour is simply a set of contour points $v(s) = (X(s), Y(s))$ parameterized by $s \in [0, 1]$. It attempts to minimize an energy associated to the current contour as a sum of the internal and external energy: $E = E_{\text{internal}} + E_{\text{external}}$, where

$$\begin{aligned} E_{\text{internal}} &= \frac{1}{2}\left(\alpha(s)|\mathbf{v}_s(s)|^2\right) + \frac{1}{2}\left(\beta(s)|\mathbf{v}_{ss}(s)|^2\right) \\ &= \frac{1}{2}\left(\alpha(s)\left\|\frac{d\bar{v}}{ds}(s)\right\|^2 + \beta(s)\left\|\frac{d^2\bar{v}}{ds^2}(s)\right\|^2\right) \end{aligned} \tag{2.1}$$

with $\alpha(s)$ and $\beta(s)$ representing some properly selected non-negative weights, and

$$E_{\text{external}} = -\int_0^1 f(X(s), Y(s))ds, \quad \text{where } f(x, y) = |\nabla I(x, y)|^2, \tag{2.2}$$

where I is the analyzed image.

The minimization of the contour energy E is solved numerically by applying the calculus of variations to (2.1) and (2.2) [22]. Thus, two independent Euler equations are obtained, which are then solved by using the finite difference method.

This parametric active contour model has some obvious limitations, such as the poor convergence performance for concave boundaries and for the case when the snake is initialized far from minimum. Also, a higher accuracy of it requires tighter convergence criteria used for energy minimization and therefore, a higher computation time.

An example of object segmentation using this snake proposed by Kass et al. is displayed in the next figure [22].

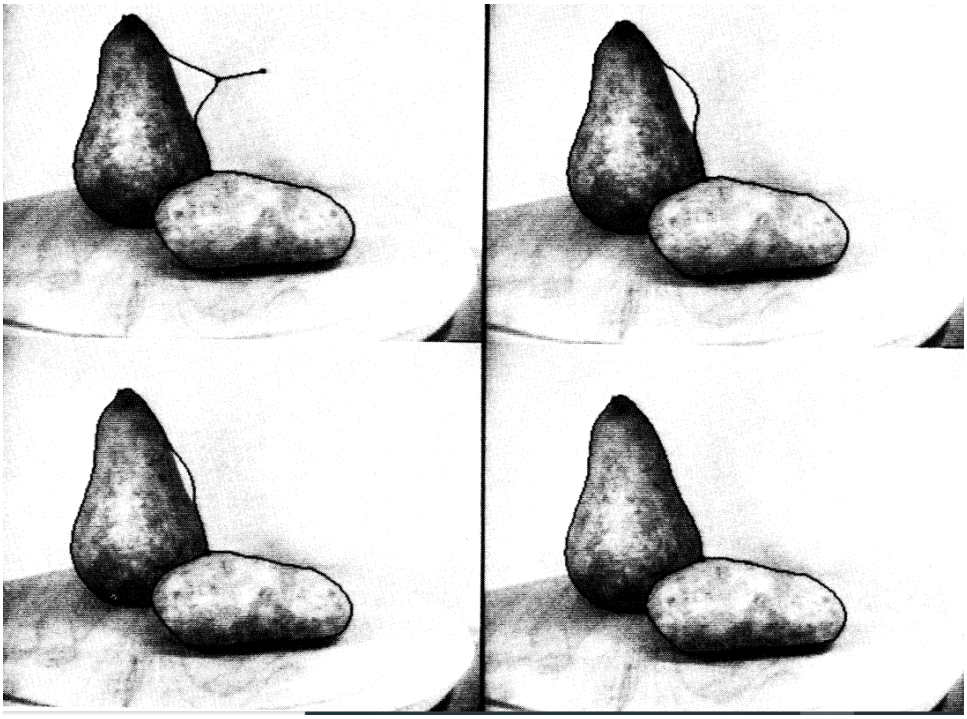

Figure 1: Snake evolving to the contours of objects representing pear and potato

Other active contour models variants that improve the default snake model have been developed in the last decades. Such a active contour model that addresses the issues of the previous model is the *Gradient vector flow* (GVF) snake model, which was introduced by C. Xu and J. L. Prince in 1997 [30].

Thus, the *gradient vector flow* (GVF) field $\mathbf{v}$ minimizes the following energy functional:

$$E_{\mathrm{GVF}} = \int\int \mu(u_x^2 + u_y^2 + v_x^2 + v_y^2) + |\nabla f|^2 |\mathbf{v} - \nabla f|^2 dx\, dy,$$

where $f(x, y)$ represents an edge map derived from $I(x, y)$.

This energy minimizing can be solved by solving two Euler equations [30]. Those equations are then solved through iteration towards a steady-state value [30].

The GVF active contour solves the poor convergence performance problems of the snake of Kass et al. Thus, the example described in the following figure prove that a snake with GVF external forces moves successfully into a concave boundary region [30].

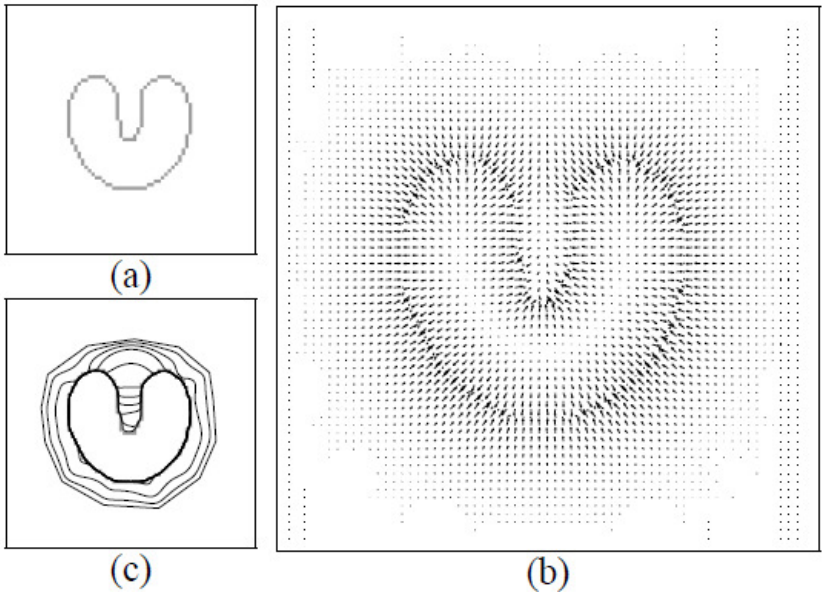

Figure 2: GVF snake moving into a concave boundary region

The *Balloon model* represents another type of active contour that has been introduced in order to overcome the limitations of the default snake model [15]. The original snake is not attracted to distant edges. Also, it shrinks inwards if no substantial images forces are acting upon it.

The Balloon model makes the curve behave like a balloon that is inflated by an additional force. The initial contour need no longer be close to the solution to converge. It passes over the weak boundaries and stops only if the boundary is strong enough.

So, the balloon active contour model introduces the following inflation term into the forces that act on the snake:

$$E_{\text{inflation}} = k_1 \vec{n}(s),$$

where k_1 represents the magnitude of the force, while $n(s)$ is normal unitary vector of the evolving curve [15].

The balloon model has its own disadvantages. Thus, the outward force makes the contour slightly larger than the actual minima. Also, the inflation force could overpower forces from the weak boundaries.

The *region-based active contours* represent another category of deformable models. The most popular region-based active contour is the piecewise-smooth Mumford and Shah model introduced in 1989 [26].

The Mumford and Shah snake model is based on the minimization of the following energy functional:

$$E(u, C) = \frac{1}{2}\int_{\Omega}(f-u)^2 dx + \lambda^2 \frac{1}{2}\int_{\Omega - C}|\nabla u|^2 dx + v\|C\|, \tag{2.3}$$

where f represents the function of the image to be segmented and $\|C\|$ is the length of the evolving contour C [26].

The variational Mumford–Shah segmentation model given by (2.3) is ill posed and difficult to solve. A large number of solutions that minimize this energy functional have been proposed in the last decades [12].

An active contour model that is based on a modified Mumford–Shah energy functional is the *diffusion snake model* [16]. This diffusion-based deformable model introduced by Cremers et. al in 2001 addresses several issues of the active contour models, such as their sensitivity to noise, clutter and occlusions.

The energy that is defined for the contour C has the following form:

$$E_i(u, C) = E_i(u, C) + \alpha \cdot E_c(C),$$

where E_c favors contours which are familiar from a learning process and the other energy term of this sum is the next modified Mumford–Shah energy functional:

$$E_i(u, C) = \frac{1}{2}\int_{\Omega}(f-u)^2 dx + \frac{1}{2}\lambda^2 \int_{\Omega - C}|\nabla u|^2 dx + vL(C),$$

where $L(C) = \int_0^1 C_s^2 ds$.

So, this represents a hybrid active contour combining the external energy of the Mumford–Shah energy functional with the internal energy of the Kass snake. The total energy E is then iteratively minimized with respect to both the segmenting contour C and the segmented image u [16, 17]. This energy minimization process leads to the Euler–Lagrange equation. Next, solving this equation by applying the gradient descent method results in a evolution equation that is approximated numerically.

Other versions of this active contour model have been also developed. One of them is the *simplified diffusion snake* [17]. An example of diffusion snake-based image segmentation is displayed in Fig. 3 describing the results of the segmentation with and without prior knowledge about object shape [16].

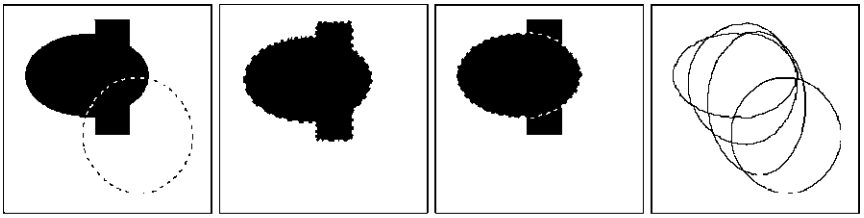

Figure 3: Image segmentation using diffusion-based snake

3 Geometric PDE-based segmentation models

The second type of variational PDE-based image segmentation models is that of geometric segmentation models. These deformable models represent contours implicitly as *level sets* of 2-D scalar functions.

Geometric (Geodesic) Active Contours (GAC), which were introduced by V. Caselles et al. in 1993, represent active contours evolving in time according to the intrinsic geometric measures of the analyzed image [13]. These GAC models are obtained by combining the parametric active contours to level-sets and represent a proper solution to address the limitations of the parametric snakes described in the previous section.

The *level set* of a real-valued function f is a set where the function takes on a given constant value c:

$$L_c(f) = \{(x_1, ..., x_n) \mid f(x_1, ..., x_n) = c\}.$$

This level-set becomes a level curve for $n = 2$, a level surface for $n = 3$ and a level hypersurface for $n > 3$. Also, if f is differentiable, the level set is a hypersurface and a manifold outside the critical points of this function. The level sets have been successfully applied to both contour-based and region-based image segmentation.

A geodesic active contour perform the following energy minimization:

$$\text{Min} \int_0^1 g(|\nabla I(C(q)|)|C\prime(q)|dq, \tag{3.1}$$

where C is a parametrized planar curve [13].

Then, one applies the Euler-Lagrange equation corresponding to (3.1) and obtains the next gradient descent curve evolution equation of GAC:

$$\frac{\partial C(t)}{\partial t} = g(I)\kappa\vec{\mathcal{N}} - (\nabla g \cdot \vec{\mathcal{N}})\vec{\mathcal{N}},$$

where κ represents the Euclidean curvature and $\vec{\mathcal{N}}$ represents the unit inward normal [13].

This geodesic flow leads to the following evolution equation:

$$\frac{\partial u}{\partial t} = |\nabla u)\text{div}\left(g(I)\frac{\nabla u}{|\nabla u|}\right) + \nu g(I)|\nabla u| \tag{3.2}$$

if C is the level-set of the function u.

The geometric active contour models have been applied successfully in the medical image computing domain. A medical image segmentation example, representing a tumor detection using a GAC model is provided in Fig. 4 [13].

These geometric active contours can be also applied to detect and track the moving objects in the video sequences [13]. A term related to the object displacement between frames can be added to the PDE given by (3.2) for this purpose:

$$\frac{\partial u}{\partial t} = |\nabla u|\text{div}\left(g(t,x)\frac{\nabla u}{|\nabla u|}\right) + \nu g(t,x)|\nabla u| + (1 - g(t,x)))v \cdot \nabla u.$$

Another type of geometric PDE-based segmentation models, also using level sets, is that of the *active contour models without edges*. Such a level-set based image

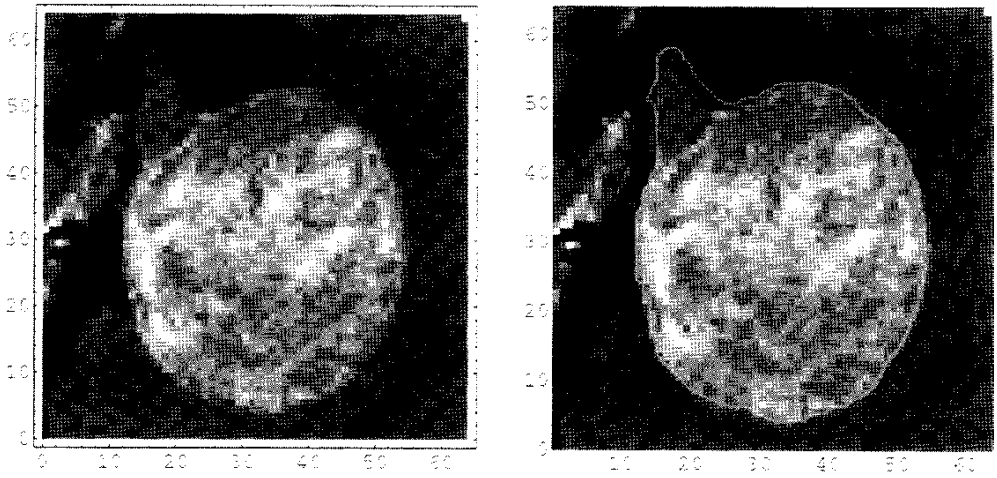

Figure 4: Tumor detection using a GAC model

segmentation approach is the well-known segmentation model introduced by Chan and Vese in 1999 [14].

The Chan–Vese segmentation model does not rely on edges at all. It represents the segmentation boundary implicitly with a level set function [14]. It is inspired by a simplified Mumford–Shah segmentation model. If f represents the image to be segmented, this variational scheme is based on the next functional minimization:

$$\arg\min_{u,C} \ \mu \ \text{Length}(C) + \int_\Omega (f(x) - u(x))^2 dx,$$

where $u(x) = \begin{cases} c_1, & \text{where } x \text{ is inside } C, \\ c_2, & \text{where } x \text{ is outside } C. \end{cases}$

Chan–Vese technique identifies among all u of this form the one that best approximates the function f:

$$\begin{aligned} \arg\min_{c_1,c_2,C} \ & \mu \ \text{Length}(C) + \nu \ \text{Area}(\text{inside}(C)) \\ & + \lambda_1 \int_{\text{inside}(C)} |f(x) - c_1|^2 dx + \lambda_2 \int_{\text{outside}(C)} |f(x) - c_2|^2 dx. \end{aligned}$$

Here C is represented as the zero-crossing of a level set function:

$$C = \{x \in \Omega : \varphi(x) = 0\}. \tag{3.3}$$

So, the Chan–Vese minimization can be rewritten as follows:

$$\begin{aligned} \arg\min_{c_1,c_2,C} \ & \mu \int_\Omega \delta(\varphi(x)) |\nabla \varphi(x)| dx + \nu \int_\Omega H(\varphi(x)) dx \\ & + \lambda_1 \int_\Omega |f(x) - c_1|^2 H(\varphi(x)) dx + \lambda_2 \int_\Omega |f(x) - c_2|^2 (1 - H(\varphi(x))) dx, \end{aligned}$$

where H denotes the Heaviside function and

$$C_1 = \frac{\int_\Omega f(x) H(\varphi(x)) dx}{\int_\Omega H(\varphi(x)) dx}, \quad c_2 = \frac{\int_\Omega f(x)(1 - H(\varphi(x))) dx}{\int_\Omega (1 - H(\varphi(x))) dx}.$$

This variational Chan–Vese model is then solved by applying a semi-implicit gradient descent method [14]. Other finite-difference based numerical implementation algorithms have been also proposed for this segmentation model.

A Chan–Vese image segmentation example proving the model does not depend on edges is described in Fig. 5. A cluster detection task is performed successfully after 6000 iterations of the Chan–Vese algorithm.

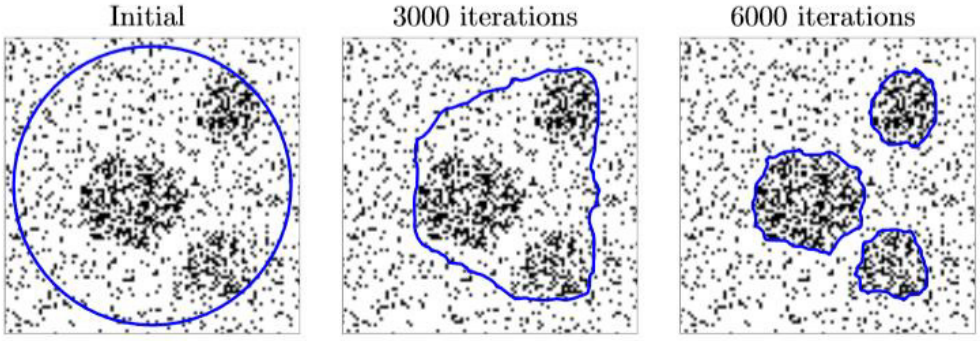

Figure 5: Cluster detection using Chan-Vese segmentation

A level-set based variational image segmentation framework has been also proposed by us in [5]. It is based on the following energy functional minimization:

$$\varphi^* = \arg\,\min\{F(vf);\ \varphi \in X(\Omega)\},$$

where

$$\begin{aligned} F(\varphi) &= \mu\int_\Omega |\nabla H(\varphi)|dx\,dy + \nu\int_\Omega H(\varphi)dx\,dy + \lambda_1\int_\Omega (u_0 - C_1(\varphi))^2 H(\varphi)dx\,dy \\ &\quad +\lambda_2\int_\Omega (u_0 - C_2(\varphi))^2(1-H(\varphi))dx\,dy + \lambda_3\int_\Omega |\varphi|^2 dx\,dy. \end{aligned}$$

This PDE variational scheme has been solved by applying a finite difference-based numerical approximation algorithm that is described in [5].

While this level-set based approach does not rely on image boundaries, another nonlinear PDE-based automatic image segmentation technique developed by us is based on edges [2]. It detects successfully the boundaries of the objects by applying a multi-scale image analysis.

The multi-scale image analysis used by the proposed framework is based on a nonlinear anisotropic diffusion-based scale-space that is constructed by applying the finite difference method-based numerical approximation scheme of a well-posed second-order partial differential equation-based model. The boundaries are detected at each scale of the obtained PDE-based scale-space by searching for zero-crossings and applying some gradient magnitude thresholding procedures and morphological operations. The edges determined at multiple scales are then combined using a fine-to-coarse edge tracking into the final edge detection output [2].

These PDE-based segmentation approaches can be applied successfully in some image analysis domains that have been widely approached by us in the past, such as object detection and tracking [6], face detection [1], and biometric recognition [3, 7].

4 Conclusions

An overview of the PDE-based image segmentation techniques has been provided in this research article. The methods described here represent variational schemes minimizing some properly chosen energy functionals.

Both parametric and geometric PDE-based image segmentation models have been described here. The parametric segmentation approaches, which have been presented first, represent various active contour models based on parametrized curves. The geometric deformable segmentation models, described next, have been introduced in order to address the limitations of the parametric snakes. They improve those parametric active contours by combining them to some level-set functions. Also, these geometric, or geodesic, active contours could segment successfully the movie sequences, detecting and tracking properly their video objects.

Our own contributions in this PDE-based image segmentation domain have been also discussed here. One of the segmentation techniques proposed by us has a variational character and is based on level sets, while another method detects the boundaries using a multi-scale analysis based on a nonvariational anisotropic diffusion model. They could be applied successfully in various image analysis and computer vision fields.

References

[1] T. Barbu, *An automatic face detection system for RGB images*, International Journal of Computers, Communications & Control 6, 1 (2011), 21-32.

[2] T. Barbu, *Automatic Edge Detection Solution using Anisotropic Diffusion-based Multi-scale Image Analysis and Fine-to-coarse Tracking*, Proceedings of the Romanian Academy, Series A: Mathematics, Physics, Technical Sciences, Information Science, 22, 3 (2021), 265-273.

[3] T. Barbu, *Comparing various voice recognition techniques*, 2009 Proceedings of the 5th Conference on Speech Technology and Human-Computer Dialogue, 2009, 1-6, IEEE.

[4] T. Barbu, *Novel Diffusion-Based Models for Image Restoration and Interpolation*, Book Series: Signals and Communication Technology, Springer International Publishing, 126 pages, 2019.

[5] T. Barbu, *Robust contour tracking model using a variational level-set algorithm*, Numerical Functional Analysis and Optimization, Taylor & Francis 35, 3 (2014), 263-274.

[6] T. Barbu, *SVM-based human cell detection technique using histograms of oriented gradients*, Mathematical Methods for Information Science & Economics: Proceedings of the 3rd International Conference for the Applied Mathematics and Informatics, AMATHI '12, Montreux, Switzerland 2012, 156-160.

[7] T. Barbu, *Unsupervised SIFT-based face recognition using an automatic hierarchical agglomerative clustering solution*, Procedia Computer Science 22 (2013), 385-394.

[8] T. Barbu, *Variational image inpainting technique based on nonlinear second-order diffusions*, Computers & Electrical Engineering 54 (2016), 345-353.

[9] T. Barbu, C. Morosanu, *Image restoration using a nonlinear second-order parabolic PDE-based scheme*, Analele Stiintifice ale Universitatii Ovidius Constanta, Seria Matematica XXV, 1 (2017), 33-48.

[10] L. Barghout, J. Sheynin, *Real-world scene perception and perceptual organization: Lessons from Computer Vision*, Journal of Vision 13, 9 (2013), 709. doi:10.1167/13.9.709.

[11] S. Belongie et al., *Color-and texture-based image segmentation using EM and its application to content-based image retrieval*, Sixth International Conference on Computer Vision (IEEE Cat. No. 98CH36271). IEEE, 1998.

[12] B. Bourdin, A. Chambolle, *Implementation of an adaptive finite-element approximation of the Mumford-Shah functional*, Numerische Mathematik 85, 4 (2000), 609-646.

[13] V. Caselles, F. Catte, T. Coll, F. Dibos, *A geometric model for active contours in image processing*, Numerische Mathematik 66, 1 (1993), 1-31.

[14] T. Chan, L. Vese, *An active contour model without edges*, International Conference on Scale-Space Theories in Computer Vision, Springer, Berlin, Heidelberg 1999, 141-151.

[15] L. D. Cohen, *On active contour models and balloons, CVGIP*, Image Understanding 53, 2 (1991), 211-218.

[16] D. Cremers, C. Schnorr, J. Weickert, *Diffusion-snakes: combining statistical shape knowledge and image information in a variational framework*, Proceedings IEEE Workshop on Variational and Level Set Methods in Computer Vision, IEEE 2001, July, 137-144.

[17] D. Cremers, F. Tischhauser, J. Weickert, C. Schnorr, *Diffusion snakes: Introducing statistical shape knowledge into the Mumford-Shah functional*, International Journal of Computer Vision 50, 3 (2002), 295-313.

[18] J. A. Delmerico, P. David, J. J. Corso, *Building facade detection, segmentation and parameter estimation for mobile robot localization and guidance*, International Conference on Intelligent Robots and Systems, 2011, 1632-1639.

[19] M. Forghani, M. Forouzanfar, M. Teshnehlab, *Parameter optimization of improved fuzzy c-means clustering algorithm for brain MR image segmentation*, Engineering Applications of Artificial Intelligence 23, 2 (2010), 160–168.

[20] S. Jianbo Shi, J. Malik, *normalized cuts and image segmentation*, IEEE Transactions on Pattern Analysis and Machine Intelligence 22, 8 (2000), 888-905.

[21] T. Lindeberg, M.-X. Li, *Computer Vision and image understanding* 67, 1 (1997), 88-98. doi:10.1006/cviu.1996.0510.

[22] M. Kass, A. Witkin, D. Terzopoulos, *Snakes: active contour models*, International Journal of Computer Vision 1, 4 (1988), 321-331.

[23] J. Kenney, T. Buckley, O. Brock, *Interactive segmentation for manipulation in unstructured environments*, In 2009 IEEE International Conference on Robotics and Automation, IEEE 2009, May, 1377-1382.

[24] Z. Liu, L. Wang, G. Hua, Q. Zhang, Z. Niu, Y. Wu, N. Zheng, *Joint video object discovery and segmentation by coupled dynamic Markov networks*, IEEE Transactions on Image Processing 27, 12 (2018), 5840-5853.

[25] H. Mobahi, S. R. Rao, A. Y. Yang, S.S. Sastry, Y. Ma, *Segmentation of natural images by texture and boundary compression*, International Journal of Computer Vision 95 (2011), 86-98.

[26] D. Mumford, J. Shah, *Optimal approximations by piecewise smooth functions and associated variational problems*, Communications on Pure and Applied Mathematics 42, 5 (1989), 577-685.

[27] D. L. Pham, C. Xu, J. L. Prince, *Current methods in medical image segmentation*, Annual Review of Biomedical Engineering 2 (2000), 315-337.

[28] L. G. Shapiro, G. C. Stockman, *Computer Vision*, Prentice-Hall, New Jersey, 2001; 279-325.

[29] L. Wang, X. Duan, Q. Zhang, Z. Niu, G. Hua, N. Zheng, *Segment-Tube: spatio-temporal action localization in untrimmed videos with per-frame segmentation*, Sensors 18, 5 (2018), 1657, https://doi.org/10.3390/s18051657

[30] C. Xu, J. L. Prince, *Gradient vector flow: A new external force for snakes*, Proceedings of IEEE computer society conference on computer vision and pattern recognition, IEEE, (1997), 66-71.

Author's address:

Tudor Barbu
Institute of Computer Science of the Romanian Academy - Iasi Branch,
Blvd. Carol I, no. 8, Iaşi, Romania,
and
The Academy of Romanian Scientists.
E-mail: tudor.barbu@iit.academiaromana-is.ro